2016

Consistency of electron scattering data with a small proton radius

Keith Griffioen
William & Mary

Carl Carlson
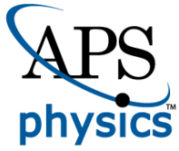*William & Mary*

Sarah Maddox
William & Mary

Recommended Citation

Consistency of electron scattering data with a small proton radius

Keith Griffioen, Carl Carlson, and Sarah Maddox

Consistency of Electron Scattering Data with a Small Proton Radius

Keith Griffioen, Carl Carlson, and Sarah Maddox

Physics Department, College of William and Mary, Williamsburg, Virginia 23187

(Dated: March 30, 2016)

We determine the charge radius of the proton by analyzing the published low momentum transfer electron-proton scattering data from Mainz. We note that polynomial expansions of the form factor converge for momentum transfers squared below $4m_\pi^2$, where m_π is the pion mass. Expansions with enough terms to fit the data, but few enough not to overfit, yield proton radii smaller than the CODATA or Mainz values and in accord with the muonic atom results. We also comment on analyses using a wider range of data, and overall obtain a proton radius $R_E = 0.840(16)$ fm.

I. INTRODUCTION

Much remains to be learned about the proton. After a half-century of study, we still do not know what its size is, where its spin comes from, and how its mass is generated from light quarks and gluons. Particularly troubling is the matter of the proton's charge radius, R_E. This was first measured to be approximately 0.8 fm by Hofstadter and collaborators in the 1950s via elastic electron scattering [1]. The value of R_E has been steadily refined over the years through electron scattering and hydrogen energy level measurements, recently reviewed in Refs. [2, 3]. The CODATA group [4, 5], using available electron-based data through 2014, quotes a combined value of $R_E = 0.8751 \pm 0.0061$. The recent electron scattering experiment in Mainz [6–8], which quotes a value of $R_E = 0.879 \pm 0.008$, is included in this CODATA value. For many years R_E had remained relatively stable at about 0.88 fm, until this value was called into question by Lamb shift measurements in muonic hydrogen, which yielded a value of $R_E = 0.84087 \pm 0.00039$ fm [9, 10]. This radius is 7 standard deviations away from the CODATA value. The proton size puzzle leaves us with three options: the hydrogen Lamb shift and elastic electron scattering experiments have erred in extracting R_E, the muon Lamb shift measurement is precise, but inaccurate, or there is new physics that affects the muon differently than the electron, rendering the theory behind the muonic Lamb shift calculations incomplete [11–16].

In this paper, we explore whether the published, high-quality ep elastic scattering data at low-Q^2 from Mainz could be consistent with the muonic Lamb shift determination of R_E. Extracting R_E from elastic electron scattering is as simple, or as difficult, as measuring the slope of the electric form factor $G_E(Q^2)$ as a function of the squared four-momentum transfer Q^2 as Q^2 goes to zero. However, since the differential cross section diverges at small scattering angles (low Q^2), these measurements are very sensitive to beam alignment and angle determination. No ep measurement extends to $Q^2 = 0$, although some get close. Mainz currently holds the record, with measurements at Q^2 as low as 0.0038 GeV^2. This modern data set, with 1422 data points in the range from the lower limit to about 0.98 GeV^2, is the best, most precise, and most extensive available. Therefore, it is the Mainz data that we choose to explore.

The charge radius is given by the second term in the expansion of the electric form factor,

$$G_E(Q^2) = 1 - \frac{1}{6}R_E^2 Q^2 + a_2 Q^4 + \dots. \quad (1)$$

Using data at very low Q^2, where the curvature terms (Q^4 and higher) give small contributions, the charge radius R_E can be reliably determined without having to model the shape of G_E over a wider range of Q^2. In the past, the size of the uncertainties on the data at very low Q^2 has meant that one could not extract an accurate charge radius without extending the data range to include not-so-low Q^2. The Q^4 term then can become noticeable, depending on how far the data range is extended. There was an early example of Simon *et al.* data [17] where the fitted coefficient of the Q^4 term was small, albeit with large uncertainty, and the extracted charge radius was also small. Using this example, some workers (*e.g.,* [18]) advocated including data at still higher Q^2 to obtain a larger curvature. This also led to a larger extracted proton radius. Including higher Q^2 does not have to mean including data at all available Q^2, and we have the example of Ref. [19] using only data with $Q^2 < 0.62$ GeV^2 ($Q < 4$ fm^{-1}).

Sick and Trautmann [20], in fact, suggest that data from 0.014 to 0.056 GeV^2 in Q^2 (or Q from 0.6 to 1.2 fm^{-1}) is most crucial for finding the proton radius. The consideration of what data range is sensitive to the proton size, given the foregoing discussion, must depend on the accuracy and precision of the data. As the data improve, the range of Q^2 needed to obtain the proton radius will decrease. With the new Mainz data now available, we will explore the possibility that we can obtain a good proton radius result using only data with a rather low maximum Q^2.

The Mainz data [6–8] data enjoy state-of-the-art radiative and Coulomb corrections. One of the three spectrometers was used as a luminosity monitor to control systematic uncertainties, and the other two spectrometers measured separate kinematic points simultaneously. The data are dominated by point-to-point systematic uncertainties from background subtractions, drift-chamber inefficiencies, normalization factors, angle determinations, and the afore-mentioned corrections. The slight leeway we have in fitting these data is to make small rescalings of the 34 normalization sets in the experiment and to enlarge the point-to-point error bars if the fluctuations of the data indicate that the quoted uncertainties are too small. We limit our form factor fits to the Mainz data set because the systematic differences between separate experiments can introduce systematic effects in global fits, and

the 1422 Mainz points already dominate the sample of world data below $Q^2 = 1$ GeV^2.

We shall advocate for fits using the 243 Mainz data points with Q^2 below 0.02 GeV^2. In addition to the general principle that using only very low Q^2 will free us from model dependence incurred in extending the fits to higher Q^2, we are also using only data from a limited number of spectrometer settings. This substantially frees the data from any drift arising from the normalization adjustments that reconciled data from different spectrometer settings, and averts overfitting of inflections or statistical fluctuations in the data that can happen when using fit functions that contain many fit constants.

In the following, Sec. II presents the formalism pertinent to our discussion; Sec. III presents the extraction and discussion of the proton radius using low Q^2 data; Sec. IV presents a fit based on the full Q^2 range of the Mainz data; Sec. V highlights our final results; and Sec. VI gives our conclusions.

II. FORMALISM

When an electron of energy E scatters from a proton at rest through an angle θ and exits with energy E', the 4-momentum transfer squared is,

$$Q^2 = -q^2 = 4EE' \sin^2 \frac{\theta}{2}. \tag{2}$$

In the Born approximation, the ep elastic scattering cross section can be written in term of the electric and magnetic Sachs form factors, $G_E(Q^2)$ and $G_M(Q^2)$,

$$\frac{d\sigma}{d\Omega} = \left(\frac{d\sigma}{d\Omega}\right)_{\text{Mott}} \frac{1}{(1+\tau)} \left[G_E^2(Q^2) + \frac{\tau}{\varepsilon} G_M^2(Q^2)\right]. \tag{3}$$

The Mott cross section is

$$\left(\frac{d\sigma}{d\Omega}\right)_{\text{Mott}} = \frac{4\alpha^2 \cos^2 \frac{\theta}{2}}{Q^4} \frac{E'^3}{E}, \tag{4}$$

α is the fine structure constant,

$$\varepsilon = \left(1 + 2(1+\tau)\tan^2 \frac{\theta}{2}\right)^{-1}, \text{ and}$$

$$\tau = \frac{\nu^2}{Q^2} = \frac{Q^2}{4M^2}, \tag{5}$$

where ν is the energy transferred by the virtual photon and M is the proton mass. Further,

$$E' = \frac{E}{1 + (2E/M)\sin^2 \frac{\theta}{2}}. \tag{6}$$

The electric and magnetic form factors at $Q^2 = 0$ are normalized to correspond to the nucleon charge in units of e and the nucleon magnetic moment in units of the proton magneton $\mu_N = e/(2M)$, such that

$$G_E(0) = 1, \quad \text{and} \quad G_M(0) = \mu_p \approx 2.793. \tag{7}$$

The dipole form factor

$$G_D = \frac{1}{\left(1 + Q^2/0.71 \text{ GeV}^2\right)^2}, \tag{8}$$

suitably normalized, has been used for many years as a benchmark approximation for both G_E and G_M. The Mainz group presents data on the cross section σ as its ratio to the cross section calculated using the dipole form factors, σ_D,

$$\frac{\sigma}{\sigma_D} = \frac{\varepsilon G_E^2 + \tau G_M^2}{\varepsilon G_D^2 + \tau \mu_p^2 G_D^2}. \tag{9}$$

From this,

$$G_E(Q^2) = G_D(Q^2) \left(\frac{\sigma}{\sigma_D}\right)^{1/2}$$

$$\times \left[1 + \tau \mu_p^2 \frac{G_M^2/(\mu_p G_E)^2 - 1}{\varepsilon + \tau \mu_p^2}\right]^{-1/2}. \tag{10}$$

For $Q^2 < 0.02$ GeV^2, the square-bracket term above (including the exponent), for reasonable values of the G_E/G_M ratio, differs from unity by no more than 140 parts per million, which is only about 1% of the effect on the cross section occasioned by the difference between the electronically and muonically determined charge radii, and as such plays no decisive role in the extraction of G_E. For general Q^2, we most often will obtain G_E using the G_E/G_M ratio obtained from recoil polarization experiments, mostly at higher Q^2. The data from JLab indicate that at least for $Q^2 < 8$ GeV^2,

$$\mu_p \frac{G_E}{G_M} \approx 1 - \frac{Q^2}{8 \text{ GeV}^2}. \tag{11}$$

Returning to low Q^2, one can use the radius expansion,

$$\mu_p \frac{G_E}{G_M} = 1 - \frac{1}{6}(R_E^2 - R_M^2)Q^2, \tag{12}$$

where R_M is the magnetic radius and

$$G_E = G_D \left(\frac{\sigma}{\sigma_D}\right)^{1/2} \left\{1 + \frac{\mu_p^2 Q^4}{12M^2} \frac{R_E^2 - R_M^2}{\varepsilon + \tau \mu_p^2}\right\}^{-1/2}. \tag{13}$$

Specifically, Bernauer et al. [6] obtain $R_E = 0.879 \pm 0.008$ fm and $R_M = 0.777 \pm 0.017$ fm from their fits. The latter is significantly smaller than most other fits, where typically R_M is similar to R_E, but none-the-less, the extraction of G_E from the data at low Q^2 is unaffected by the spread of suggested values for R_M even at the high level of accuracy needed for the present investigation.

III. ANALYSIS FOR $Q^2 < 0.02$ GEV^2

Looking only at data for Q^2 below 0.02 GeV^2, there are a plethora of data points from the Mainz experiment. In this Q^2

range, the term in brackets in Eq. (10) is, for all practical purposes, unity. Mainz has 243 data points for $Q^2 < 0.02\,\text{GeV}^2$. Limiting consideration to only spectrometer B to minimize cross calibration uncertainties, still leaves 209 data points. Although the overall normalization may be uncertain by 1–2%, any relative systematic uncertainties that could lead to a false Q^2 dependence are thought to be small.
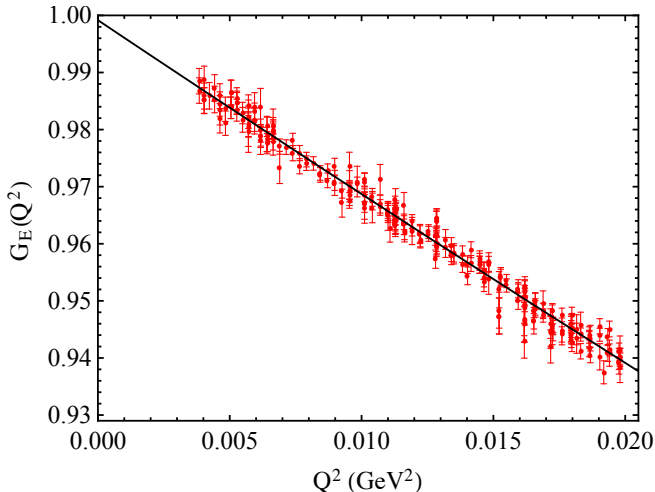

FIG. 1: (Color online) Linear plus quadratic fit to all Mainz (2010) data with $Q^2 < 0.02\,\text{GeV}^2$.

We can fit the data using a linear plus quadratic in Q^2 form for G_E,

$$G_E(Q^2) = a_1(1 + a_2 Q^2 + a_3 Q^4), \qquad (14)$$

where $a_2 = -R_E^2/6$. Using all available points below 0.02 GeV^2 gives the result shown in Fig. 1. The χ^2 per degree of freedom (dof) for the fit is 1.00, the normalization constant is 0.9992 ± 0.0003, $R_E = 0.850 \pm 0.019$ fm, consistent with the Lamb shift results, and $a_3 = 4.5 \pm 5.6\,\text{GeV}^{-4}$. The central value of a_3 is positive as one might expect from a nonrelativistic expansion of the form factor, but is statistically consistent with zero.

We mimicked the data set in Fig. 1 by generating Monte Carlo events with an exponentially falling distribution. Fits using Eq. (14) generated the correct slope with an unbiased statistical variation, but a_3 was slightly low, absorbing the contributions from higher-order curvature. This gives us confidence that the extracted slope is not biased by the curvature for samples with $Q^2 < 0.02\,\text{GeV}^2$.

Without prior expectations, one could use a rule of thumb for fitting, namely to discard terms in the fit that do not improve the χ^2/dof. A linear fit, $G_E(Q^2) = a_1(1 + a_2 Q^2)$, leads to the same χ^2/dof = 1.00, and values $a_1 = 0.9986 \pm 0.0003$ and $R_E = 0.835 \pm 0.003$ fm (using the diagonal term in the error matrix). From a statistical viewpoint, a radius as large as 0.88 fm is unfavored. However, the correlations are such that the more positive the curvature, the larger the extracted proton radius.

Fits like the ones just presented have been criticized because of expectations that the curvature could be larger than the apparent results from the quadratic fit and certainly not

zero as in the linear fit. To investigate the effects of curvature when fitting a low-Q^2 data set, we expand the electric form factor as

$$G_E(Q^2) = 1 - \frac{1}{6}R_E^2 Q^2 + \frac{b_2}{120}R_E^4 Q^4 - \frac{b_3}{5040}R_E^6 Q^6, \qquad (15)$$

where the coefficients are suggested by nonrelativistic models, R_E is the rms proton radius, $R_E^2 = \langle r^2 \rangle$, $b_2 = \langle r^4 \rangle / \langle r^2 \rangle^2$, and $b_3 = \langle r^6 \rangle / \langle r^2 \rangle^3$. The coefficients can be calculated using exponential, Gaussian, and uniform model distributions $\rho(r) = \rho_0 e^{-r/a}$, $\rho(r) = \rho_0 e^{-r^2/b^2}$, and $\rho(r) = \rho_0 \theta(c - r)$. For these three cases, respectively, $b_2 = 5/2$, $5/3$, and $25/21$, and $b_3 = 35/3$, $35/9$, and $125/81$. Although these coefficients were calculated non-relativistically and hence are approximate, they do give a range of estimates of the effects of higher-order terms on the extraction of R_E. The fits using $Q^2 < 0.02\,\text{GeV}^2$ data yield $R_E = 0.859(3)$, $0.851(3)$, and $0.846(4)$ fm, respectively, each with a χ^2/dof = 1.00. One of these results is almost neutrally between the muonic and electronic radius values, while the Gaussian and uniform distributions, even with the pre-chosen curvature terms, give results commensurate with the muonic Lamb shift value.

The fit just discussed is one example. One may inquire what results follow with different Q_{max}^2 (always with $Q_{max}^2 < 4m_\pi^2$) and different orders of polynomial. There will be two criteria for an acceptable fit. One is that the χ^2 is low enough, on the order of 1 per degree of freedom. The other is that the highest order term in the polynomial is not well determined, as judged by the uncertainty limit on its coefficient, with the previous terms well determined. This will imply that the fit has omitted no important term, and is good. Fig. 2 shows χ^2/dof and R_E from a number of linear, quadratic, and cubic (in Q^2) fits, with the small numbers indicating Q_{max}^2 for each example in multiples of 0.01 GeV^2.

The linear fits cannot sensibly satisfy the second criterion and still give a radius, but they are included to show what happens when Q_{max}^2 increases and the number of terms in the fit does not. The diagonal elements of the error matrix are astonishingly small, but the fits are poor, as judged by χ^2. Three quadratic fits are shown, with Q_{max}^2 indicated on the Figure. The lowest one is our prime example, which satisfies all criteria. It has an acceptable χ^2 and a small contribution from the actual Q^4 term in the polynomial. The next still has an acceptable χ^2, but the coefficient of the Q^4 term is stringently determined (circa 10% uncertainty), leading to worries that a cubic expansion is not flexible enough for this Q_{max}^2, and so should not be trusted. The last point in this series sees some rise in χ^2, and with tightly determined coefficients again indicating underfitting at this Q_{max}^2. For the two cubic fits shown, the one with lower Q_{max}^2 reasonably satisfies the criteria, while the upper one has its Q^6 coefficient tightly determined, again indicating underfitting. Quartic fits did not give suitable results with Q_{max}^2 limited by the $\pi\pi$ threshold. Some Q_{max}^2 values, although happening to give an R_E that matches the muonic hydrogen results, leads to fits with several poorly determined coefficients, and for other Q_{max}^2 the sign pattern of the coefficients does not match the alternation expected for smooth charge distributions and the Fourier transform formula. The
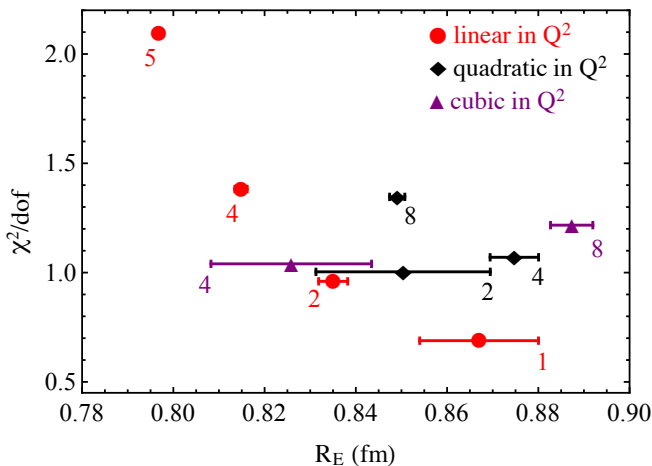
FIG. 2: (Color online) χ^2/dof vs. R_E for polynomial fits to the data set, showing fits with first, second, and third order polynomials in Q^2 using data with $0.01 < Q^2_{max} < 0.08$ GeV^2. The small numbers near each data point gives Q^2_{max} in multiples of 0.01 GeV^2. A good fit should have a good χ^2 and a sufficient but not oversufficient number of parameters, as further discussed in the text. The quadratic fit "2" and the cubic fit "4" satisfy the criteria.

overall conclusion from further examinations of fits to the the low Q^2 range of the data, is that when the criteria for good fits are satisfied, the proton radius accords with the muonic hydrogen value.

IV.   THE FULL Q^2 RANGE

We have so far concentrated on using low-Q^2 data to obtain the proton radius, but there is interest in considering the full data set. There are several topics to discuss. Can a smooth function, with relatively few parameters give an acceptable fit to the data, and what is the radius that follows from such a fit? What is the value and effect of fitting with more parameters? With more parameters one can fit systematic deviations or statistical fluctuations from what is really smooth data, which can mar the overall fit and skew the extrapolation to the proton radius. Also, with more parameters, there is a tendency for extensions outside the fit region to rapidly deviate from a properly smooth continuation of the data, with particular impact on extracting the charge radius when the deviations are in the low-Q^2 region.

Another item to consider is that the polarization method for obtaining the form factors has shown that G_E falls relative to G_M with increasing momentum transfer, approximately as $\mu_p G_E/G_M = 1 - Q^2/(8 \text{ GeV}^2)$ [21–25]. We used this earlier when obtaining G_E from the cross section data. For low Q^2 data the difference between G_E obtained using the polarization results and using scaling, $\mu_p G_E = G_M$, is minor. However, the full range of the Mainz data gives unexpected support for the polarization result. This is surprising, considering that it is a Rosenbluth experiment without hard two-photon corrections, while all earlier Rosenbluth results gave scaling

($\mu_p G_E/G_M \approx 1$). Also in the absence of two-photon corrections, a reduced cross section at fixed Q^2 should be linear in ε (see Eq. (3)). Two-photon corrections change the slope in ε, and may also give some ε^2 and higher dependence, which will be sought in the data in the ensuing subsections.

A.   Full Range Fit

For our analysis of the full data set, we have chosen a continued fraction (CF) form

$$f(Q^2) = \cfrac{c_1}{1 + \cfrac{c_2 Q^2}{1 + \cfrac{c_3 Q^2}{1 + \cfrac{c_4 Q^2}{1 + ...}}}}, \tag{16}$$

for $G_E(Q^2)$, in which $c_2 = (R_E/\hbar c)^2/6$. A truncated continued fraction is a ratio of polynomials, and it resembles Padé approximates. The continued fraction could be dangerous, because it can have singularities in the spacelike region whenever one of the constants c_i is negative. However, if singularities do not occur within the fit range, the continued fraction is acceptable, and it allows a wide range of shapes covering several orders of magnitude with relatively few parameters. On the other hand, fit functions with few parameters are unable to capture small inflections in the data. Since there is no theoretical restriction that forbids inflections, many people believe that they should exist. We have looked for inflections in the data, and we find no persuasive argument to include them in our parameterization. The low-Q^2 expansion of the continued fraction is

$$\begin{aligned} f_{lowQ}(Q^2) &= c_1[1 - c_2 Q^2 + c_2(c_2 + c_3)Q^4 \\ &\quad - c_2((c_2 + c_3)^2 + c_3 c_4)Q^6 + ...]. \end{aligned} \tag{17}$$
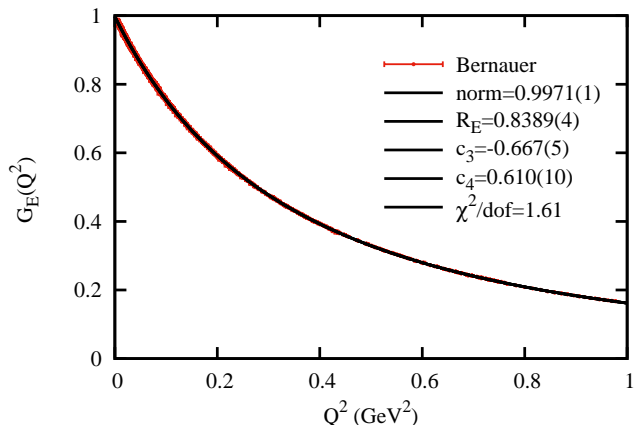

FIG. 3: (Color online) Four-parameter continued fraction fit to the full Mainz data set using $\mu_p G_E/G_M = 1 - Q^2/(8 \text{ GeV}^2)$.

We extracted G_E vs. Q^2 using Eq. (10) and fit all data to a 4-parameter continued fraction form. Adding a fifth parameter did not improve the fit, so we limited ourselves to 4 parameters. The χ^2/dof is 1.6, which is high, and we shall

have more to say about this later. However, the data are well-fit on average in all regions of Q^2. From this fit we obtain $R_E = 0.8389 \pm 0.0004$. The uncertainty on R_E is small because a constraining fit form introduces information into the problem, in this case a belief in smoothness, which is in turn reflected in the small diagonal uncertainties. Said another way, if the form factor can be faithfully described with a continued fraction with only a few terms, then R_E is tightly constrained. But does the limited freedom of the continued fraction fit inappropriately force a small value of R_E? We shall also discuss choosing other forms that may drive R_E one way or the other, especially if we allow undulation in an otherwise smoothly falling form factor. We note that our value for R_E is consistent with the analyses of the Mainz data by Lorenz *et al.* using theoretically motivated analytic forms for G_E [26, 27], although these fits have been criticized[50].

The coefficient of the Q^4 term (7.06 GeV^{-4}) from the CF fit, obtained from Eq. (17), is in accord with the result of the analysis using only low-Q^2 data. Furthermore, the contribution of the Q^6 term from the CF fit is less than 0.00005 for Q^2 below 0.02 GeV^2, and so it has negligible impact there.

We are able to fit the residuals in Fig. 3 to a sum of 8 Gaussians, which reduces the overall χ^2/dof from 1.6 to 1.3. This shows the existence of 1–3σ systematic variations in the data with respect to a smooth, monotonically falling function. Given the small magnitude, the similar size, and the great number of these deviations, we favor the hypothesis that they are not real, and any fit should average over them.

B. G_E/G_M

We have extracted G_E assuming that $\mu_p G_E/G_M = 1 - Q^2/Q_0^2$ for $Q^2 = 8$ GeV^2, and now wish to investigate consequences of different choices for G_E/G_M, a least to the extent of considering other choices for Q_0^2. Fig. 4 shows the resulting χ^2/dof for various values of Q_0^2 upon fitting the 1422 data points with a 4-parameter CF function. The full data set favors a value of $Q_0^2 \approx 8$ GeV^2. This is bounded sharply on the low side and weakly on the high side. The numbers shown beside each point are the values of the extracted radius R_E which are only slightly influenced by the G_E/G_M ratio used to extract G_E from Eq. (9). Moreover, the radius $R_E = 0.84$ fm is stably reproduced for $4 < Q_0^2 < 20$ GeV^2. In particular, for steeper $\mu_p G_E/G_M$ slopes, the extracted R_E actually decreases slightly. This is a result rather different from Bernauer *et al.*, who obtain a larger radius and $\mu_p G_E/G_M = 1 - Q^2/(1.4 \text{ GeV}^2)$ at very low Q^2.

Fig. 5 shows the world's polarization transfer data [21–25, 28–33] for $\mu_p G_E/G_M$ on the proton (over a somewhat wider range than we have considered in the bulk of this paper). It also shows the fit we have used, and two other fits. Incidentally, fitting the form $g(Q^2) = 1 - Q^2/Q_0^2$ just to the data gives $Q_0^2 = 8.02 \pm 0.05$ with χ^2/dof = 2.3. Although the recoil polarization method is the best way we know to determine the electric to magnetic form factor ratio, being relatively free of two-photon effects, the data points below $Q^2 \approx 0.8$ GeV^2 disagree with each other more than their quoted uncertainties
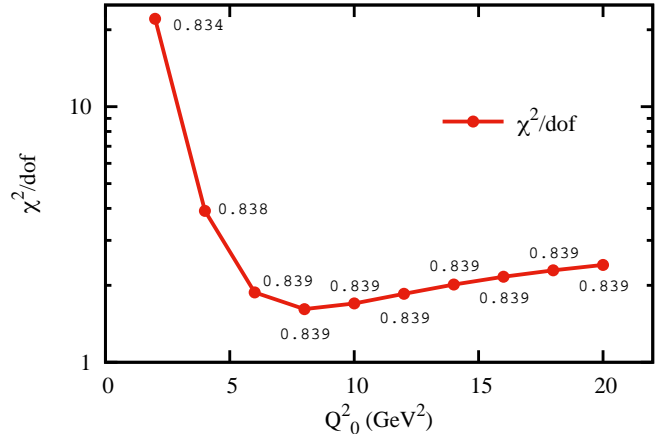

FIG. 4: (Color online) Minimum χ^2/dof values for continued fraction fits of G_E extracted using $\mu_p G_E/G_M = 1 - Q^2/Q_0^2$ with different values of Q_0^2, when using the Mainz data. Each point shows the value of R_E extracted for a given Q_0^2. The quantity R_E remains stable over the wide range $4 < Q_0^2 < 20$ GeV^2, indicating that R_E is not sensitive to the *Ansatz* for G_E/G_M.

would allow. The variate $u_i = [(\mu_p G_E/G_M)_i - g(x_i)]/\sigma_i$ has a small mean of 0.02 and a large standard deviation of 4.0. From this we conclude that a linear fit acceptably represents the average of the data points, despite their underestimated uncertainties.

That the Mainz data also prefer $Q_0^2 = 8$ GeV^2, consistent with the recoil polarization data, leads to a conundrum. Earlier Rosenbluth results gave scaling. The drop in G_E/G_M with increasing Q^2 was a great surprise when announced in 1999 and published in 2000 [21]. Why the Mainz data, without full hard two-photon corrections, agree with the polarization results is a mystery.

C.   Epsilon Dependence

Fig. 6 shows G_E versus ε, for the Mainz data, for varying Q^2. There are 6 sets of points corresponding to the different beam energies of the experiment. Since G_E is a function of Q^2 (and the G_E obtained from data will reflect this if all corrections are made), a horizontal line on this plot intersects the values of ε represented by points at fixed Q^2. Likewise, a vertical line on the plot shows different values of Q^2 at constant ε. The large range in ε covered allows us to determine G_E/G_M, as discussed earlier. It is also possible that some of the apparent ε dependence can be attributed to mismatches from systematic effects in the data from different beam energies.

Fig. 7 shows the data set plotted versus ε for 20 bins in Q^2. To ensure a common Q^2 for each horizontal line in this plot, data within a given Q^2 bin were evolved to a central Q^2 using the fit $f(Q^2)$:

$$G_E(Q^2_{\text{average}}) = G_E(Q^2_{\text{measured}}) \frac{f(Q^2_{\text{average}})}{f(Q^2_{\text{measured}})}. \quad (18)$$
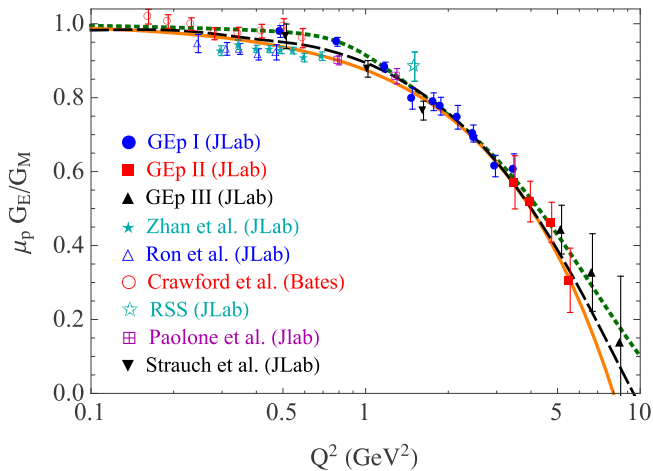
FIG. 5: (Color online) Fits to world polarization transfer data. The data are from GEp I [21, 24], GEp II [22, 23], GEp III [25], Zhan *et al.* [30], Ron *et al.* [28], Crawford *et al.* [34], RSS [35], Paolone *et al.* [36], and Strauch *et al.* [37]. Some data with larger uncertainty limits have been omitted. The solid orange line uses $\mu_p G_E/G_M = 1 - Q^2/Q_0^2$ with $Q_0^2 = 8.02$ GeV^2, the black dashed line is the Bernauer *et al.* [6–8] fit up to about 0.3 GeV^2 and a hybrid produced by other Mainz workers beyond that [38], and the green
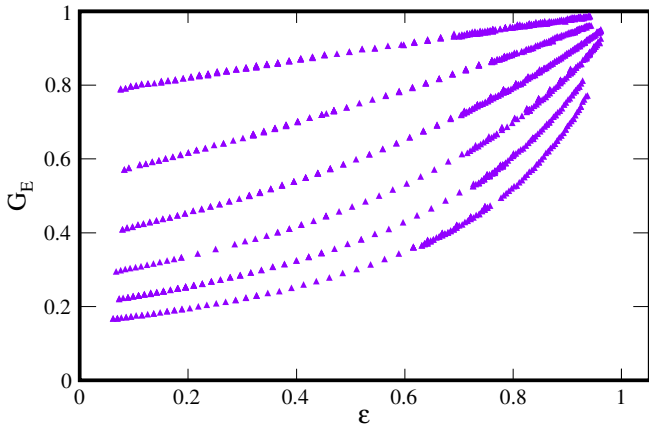

FIG. 6: (Color online) G_E vs. ε. The six sets, from top to bottom, correspond to the six beam energies of the experiment, 180, 315, 450, 585, 720 and 855 MeV.

The lines in Fig. 7 look very flat, and the actual slopes of the data in Fig. 7 are shown in Fig. 8. On average, these slopes are zero, but there are small variations. At low Q^2, G_M barely contributes to the cross section, so any ε-slope there must be an indication of mismatches in the data taken at different beam energies. The slopes are never more than a fraction of a percent, which can easily be accounted for by systematic variations in the data. Two photon effects are not expected to be appreciable at low Q^2.

D. Two Photon Contributions

A possible cause of real ε-dependence stems from two-photon exchange effects. Although the Mainz data set includes Coulomb corrections following McKinley and Fesh-
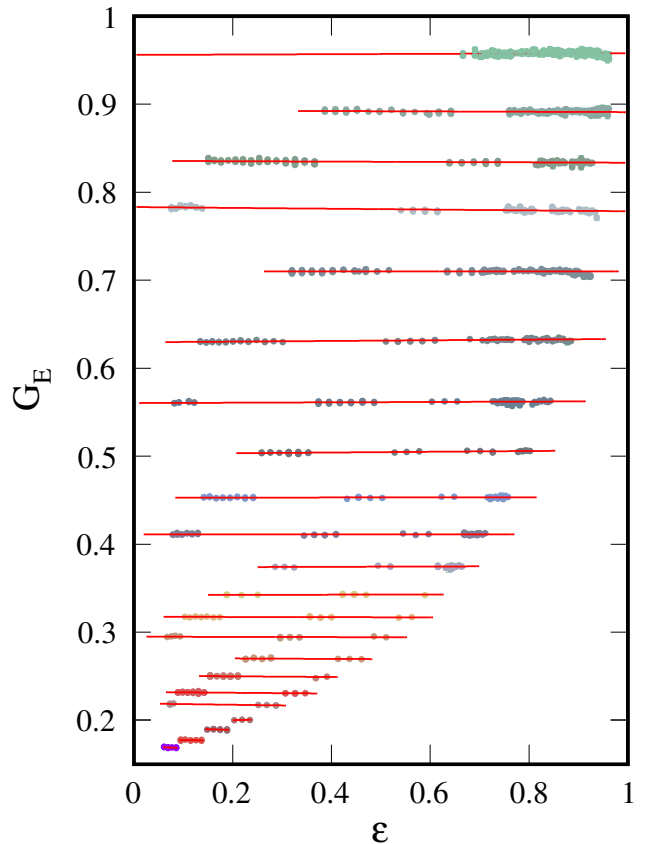

FIG. 7: (Color online) Dependence of the extracted G_E values on ε for 20 bins in Q^2. The data show little or no dependence on ε within statistics. (If desired, the actual Q^2 values may be inferred from the next Figure.)
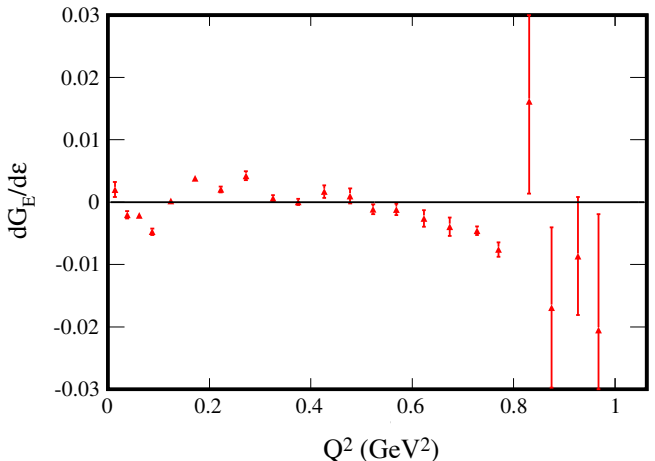

FIG. 8: (Color online) ε slopes for 14 bins in Q^2.

bach [40], which are for the limit of very heavy pointlike protons, there are further hard two-photon effects occasioned by the hadronic structure of the proton [41–43].

Recent data on the cross section ratio of positron to electron elastic scattering from the proton verifies the idea that the Rosenbluth extraction of the G_E/G_M ratio receives significant corrections from two-photon exchange [44, 45].

A potential further consequence of two photon exchange is

that in addition to changing the ε slope in the reduced cross section $G_M^2(Q^2) + (\varepsilon/\tau)G_E^2(Q^2)$, there could also be terms quadratic or higher in ε [46]. However, the data show that any ε^2 terms are small. We conclude that two-photon corrections, although they have been demonstrated to exist [47, 48], do not induce strong curvature in the Rosenbluth plot or bias the data in such a way as to change the radius R_E if one does not have data over the full range of ε.

E.   Fitting with Polynomials

The continued-fraction fit has only a few parameters and may not accurately describe inflections, if there are physical inflections, of the measured form factor. In this subsection, we experiment with other fits to the full range of the Mainz data. We consider five different generic types of fit functions, in addition to the CF fit already presented, and will show some comparison of the different fits in Fig. 9. See also [49–54].

First, for reference, we fit the whole data set to a dipole form $a_0(1 + Q^2/a_1)^{-2}$. Although the χ^2/dof is larger than acceptable at 2.28, the fit visually is remarkably good, and $R_E = 0.8299 \pm 0.0002$ fm. The dipole is famous for giving a small radius when fit to a long data set, although this value is intriguingly close to the muonic hydrogen Lamb shift value of 0.841 fm.

Second, we have followed the lead of Bernauer *et al.* [6] and fit to a double dipole $f_{dd}(Q^2) = a_0[a_1(1 + Q^2/a_2)^{-2} + (1 - a_1)(1 + Q^2/a_3)^{-2}]$. The fit has χ^2/dof = 1.6—the best, apparently, that we can achieve with a smoothly and monotonically falling fit function—and $R_E = 0.859 \pm 0.001$ fm.

Third, we consider polynomial fits. We do not advocate using polynomial fits beyond the spacelike reflection of the $\pi\pi$ threshold, since convergence of the fit is not assured beyond this point. However, they have been used elsewhere, and we would like to comment on the results. Polynomial fits with sufficient terms offer flexibility to fit inflections in the data, but they inevitably diverge outside any fit region, and accuracy at the end points is often poor for global fits.

Fourth, we consider inverse polynomials $a_0/(1 + \Sigma_{i=1}^{N} a_i Q^{2i})$.

Fifth, we consider power series expansions in $z(Q^2)$, $f_{HP}(z) = a_0(1 + \Sigma_{i=1}^{N} a_i z^i)$, as advanced in this context by Hill and Paz [55], where

$$z(Q^2) = \frac{\sqrt{4m_\pi^2 + Q^2} - 2m_\pi}{\sqrt{4m_\pi^2 + Q^2} + 2m_\pi}. \quad (19)$$

The mapping to z is motivated because a polynomial expansion of the form factor in z converges for all spacelike Q^2, as long as the cuts or poles in the form factor are at timelike q^2 with $q^2 \geq 4m_\pi^2$.

Fig. 9 shows a visual comparison of five fits: the dipole fit, the double dipole fit, and representatives of the other three fit types. The curves correspond to the differences between each model tested and the 4-parameter continued fraction (CF) fit described earlier. All polynomial fits show multiple oscillations around the CF value. Moreover, the curves are clearly
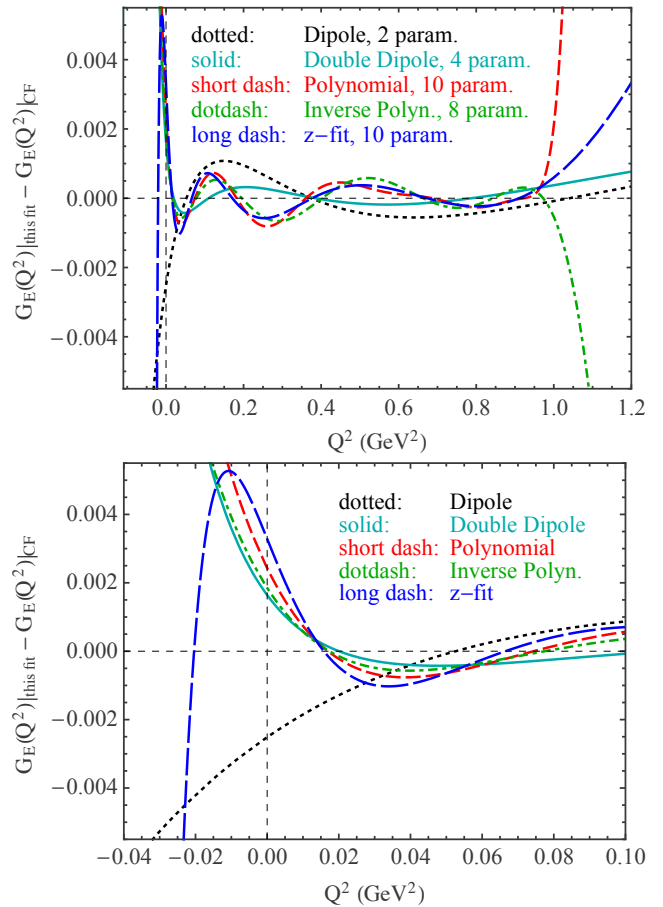

FIG. 9: (Color online) Differences between various fit forms and the standard continued fraction fit. All the power-series fit forms show undulations when enough parameters are included. The χ^2/dof drops accordingly to about 1.37, but at the expense of erratic behavior at the origin and above $Q^2 = 1$ GeV^2. The lower panel expands the low-Q^2 region of the upper panel.

unstable near $Q^2 = 0$ and $Q^2 = 1$ GeV^2, that is to say, just outside the region where the fitted data have support. With sufficient parameters, the polynomial, inverse polynomial, and z-fits all start to reproduce inflections in the data, and they track each other roughly. The large rise at $Q^2 = 0$ is the reason these fits give a larger radius than the CF fit. Although in absolute terms, the fits differ from each other by less than the point-to-point uncertainties on the data, and absolutely less than 0.001, the precise behavior of the fit function at the origin significantly influences the extracted value of R_E. Fitting fluctuations with high-order polynomials can spell trouble for extrapolations to $Q^2 = 0$, because a reduction in χ^2 likely comes at the cost of more strength in one or more of the higher-order terms, which diverge quickly outside the fit region.

F.   Systematic Deviations Between Fit and Data

The typical quoted uncertainty on each point is a few tenths of a percent. Since these data represent 34 separately normal-
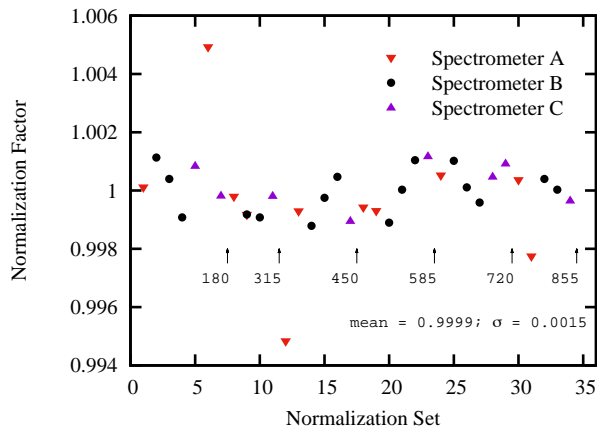
FIG. 10: (Color online) Renormalization constants for the 34 Mainz normalization sets. Red inverted triangles, black dots, and purple upright triangles correspond to Spectrometers A, B, and C, respectively. The numbers are the 6 beam energies in MeV, and the points to the left of the corresponding arrow are the sets at that energy. The average and standard deviation of these normalization constants are 1 and 0.015%, respectively.

ized data sets taken with three spectrometers, it is not unreasonable to suppose that some of the apparent undulation could be modified or removed by relative renormalization. Since absolute normalizations in each spectrometer are not known to better than a percent, there is some freedom to do this on the level of at least a few tenths of a percent.

These sorts of relative renormalizations were made by Bernauer *et al.*, with slightly different renormalizations for the different fit functions they used. We did a similar process using the continued fraction fit. For each normalization set we formed the uncertainty-weighted average of the ratio $G_E(Q_i^2)/f(Q_i^2)$ for all points in each subset. The data were then divided by this ratio. These factors are shown in Fig. 10 for the various data sets. Arrows indicate the beam energy of the points to the left of the arrow. The overall renormalization is unity, with a point-to-point variation of about 0.15%. This indicates that the original normalizations were done well, although they could be be modified a bit when using a different fit function.

To make it easier to see any systematic effects within this thicket of renormalization ratios, we combined points from different spectrometer settings within the full data sample into 14 bins of Q^2 with roughly 100 points in each bin. Fig. 11 shows the results of this exercise before the renormalizations were done (top) and after (bottom). Each plot shows the uncertainty-weighted averages of $G_E(Q^2) - f(Q^2)$, in which the uncertainties include both point-to-point statistical and systematic uncertainties. There are what appear to be statistically significant variations in $G_E(Q^2) - f(Q^2)$ in the upper plot. In fact, focusing on the low-Q^2 behavior, the data show a trend favoring a larger slope, and a bigger radius R_E, than our fits suggest. However, it is worth noting that these variations are on the order of 0.1%, which is commensurate with the point-to-point uncertainties. In the lower plot, the systematic variations seen in the upper plot are reduced by half, but
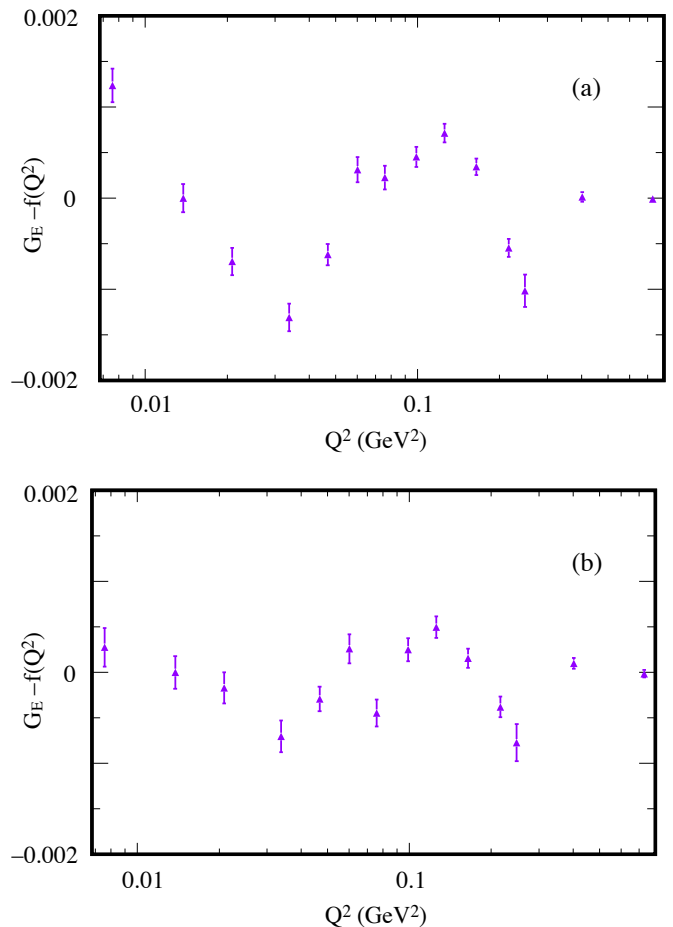

FIG. 11: (Color online) Average differences $(G_E)_i - f(Q_i^2)$ for 14 Q^2 bins before (a) and after (b) the 34 data sets. renormalizing.

renormalization cannot account for the remaining fluctuations which are on the order of 0.001.

Fig. 12 separates $G_E(Q^2) - f(Q^2)$ into plots for each spectrometer individually. Here there is a gradual rise and fall—albeit on the level of a tenth of a percent—in $G_E(Q^2) - f(Q^2)$ for Spectrometers A and C. For Spectrometer B, which is the workhorse at low Q^2, there is no such variation. Any deviations in the data from the continued fraction fit should show up in all three spectrometers if they are real. Because this is not the case, the observed fluctuations likely are not intrinsic to G_E.

We remind ourselves that the 4-parameter continued fraction fit to the full 1422-point Mainz data set is now somewhat improved by the renormalizations. After the renormalizations, R_E does not change appreciably, but the χ^2/dof decreases to about 1.4, which by some measure is still too large. Consequently, we need to consider increasing the size of the uncertainty limits.

V. FINAL RESULTS

The systematic deviations from the CF fit shown in Fig. 12 differ considerably from spectrometer to spectrometer, sug-
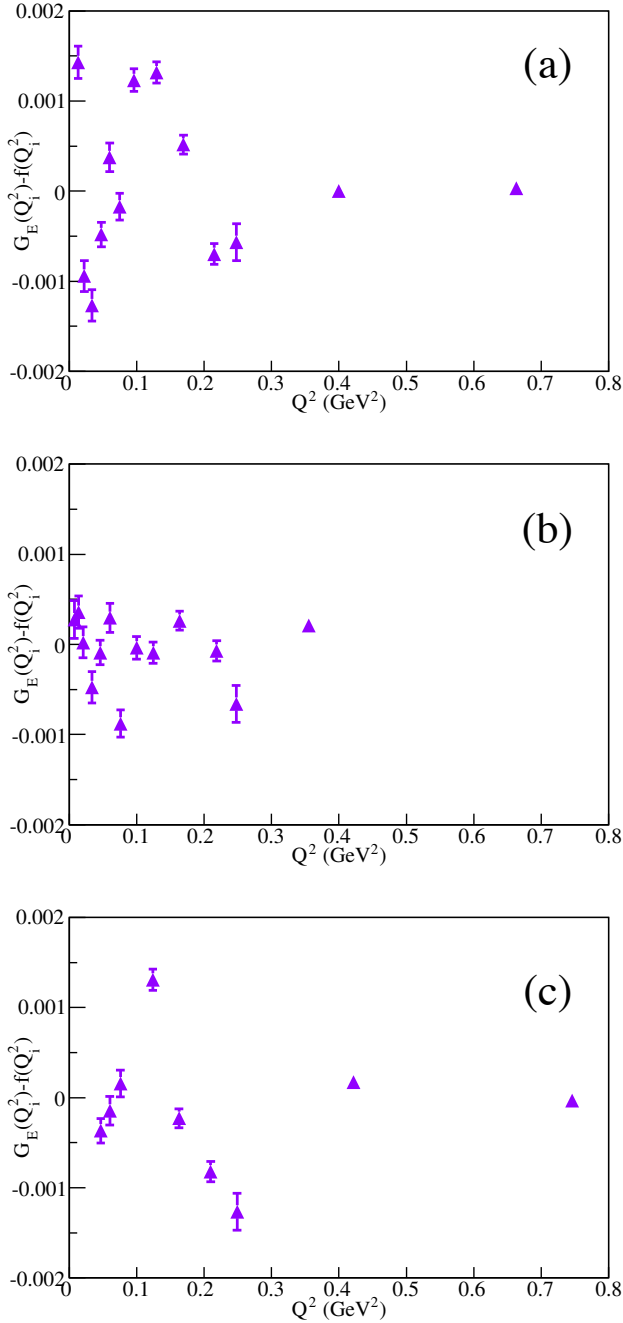
FIG. 12: (Color online) Differences, $G_E(Q_i^2) - f(Q_i^2)$, averaged over 14 Q^2 ranges for Spectrometers A (a), B (b), and C (c), individually, after renormalizations of the 34 subsets.

renormalizations of data sets and uncertainties. The resulting new fit (Fig. 13) has a χ^2/dof of unity for the full data set. All of the modifications we have made to the data have not changed R_E more than a few parts per thousand. We obtain the value $R_E = 0.8404$ fm, from this procedure, with a diagonal uncertainty of 0.00007 fm. The value of R_E fm remains consistent with the muonic hydrogen Lamb shift measurements.
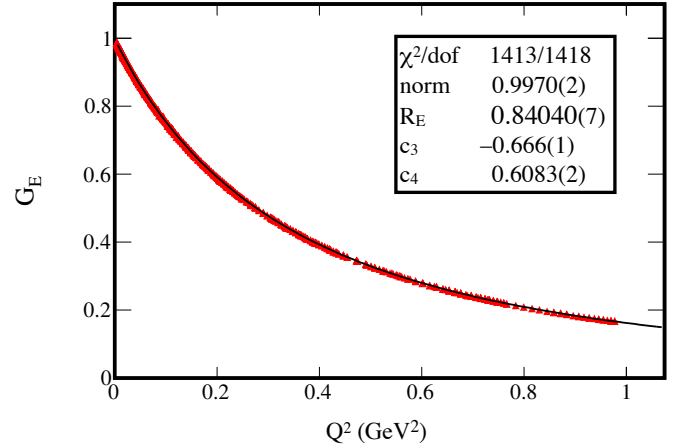

FIG. 13: (Color online) Final global fit with the 34 data sets renormalized and the point-to-point uncertainties on G_E scaled up by 15%.

Regarding the size and distribution of the uncertainties, the across-the-board increase of the uncertainty limits on G_E by 15% yields a normal distribution for $[G_E(Q_i^2) - f(Q_i^2)]/\sigma_i$. Fig. 14 shows the resulting histogram of this quantity for all 1422 points in the data set. A Gaussian fit yields a mean of zero and a standard deviation of 1 with a good χ^2/dof, as expected for Gaussian statistics.
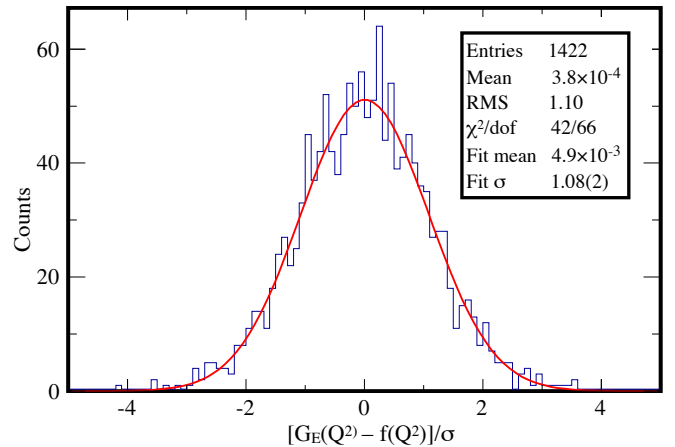

FIG. 14: (Color online) Distribution of $[G_E(Q_i^2) - f(Q_i^2)]/\sigma_i$ for all data points. Here the individual uncertainties on each point, σ_i, have all been rescaled by a factor of 1.15.

The statistical uncertainty from the χ^2 fit is small, and the overall uncertainty on R_E is dominated by systematics. We have estimated the systematic uncertainties by finding the spread among a set of extracted radii: 1) Spectrometer B,

gesting that they are not intrinsic to $G_E(Q^2)$ and perhaps that the point-to-point systematic uncertainties are underestimated. Bernauer *et al.* themselves have rescaled the uncertainties per normalization set by factors ranging from 1.07 to 2.3 [7]. Therefore, we repeated this exercise globally for $G_E(Q^2)$, and found that the uncertainties required rescaling by a factor 1.15. Fig. 13 shows the full data-set including our

$Q^2 < 0.02$ GeV^2, fits to terms up to Q^6 constrained by assuming an exponential, Gaussian, or empirical charge distribution: 0.836, 0.849, and 0.859 fm, respectively; 2) $Q^2 < 1.0$ GeV^2, fits to the double dipole, continued fraction, and inverse polynomial fit forms: 0.830, 0.840, and 0.870 fm, respectively; and 3) a global fit to the 1422 points with each of the 34 normalization constants as free parameters, 0.827 fm (not reported in detail here). The average and standard deviation within this set are 0.844 fm and 0.016 fm. We take this standard deviation as an estimate of the systematic uncertainty on R_E from fit-model dependence, and keeping the central value from our previous analysis, conclude that $R_E = 0.840 \pm 0.001_{stat} \pm 0.016_{syst}$.

VI. CONCLUSIONS

The Mainz data set is of extremely high quality—expansive, accurate, and self-consistent. We began with an analysis of the low-Q^2 part of the data set, where a polynomial expansion of the form factors should converge, and which should and does yield an accurate result for the proton radius. We found a proton radius in agreement with the muonic hydrogen Lamb shift results and significantly smaller than the CODATA value.

We also analyzed the full data set, assuming that G_E is monotonically falling and inflectionless, and used a continued fraction form to map this. We rescaled the different data sets on a level that is smaller than the original normalization uncertainties. We inflated the point-to-point systematic uncertainties by 15%, which is well within reasonable systematic uncertainties for such an electron scattering experiment.

We can then fit all data nicely using only 4 parameters. This results in a χ^2/dof of unity, and with some further consideration of other ways to fit the data, determine a proton radius $R_E = 0.840 \pm 0.016$ fm.

This result is in excellent agreement with the muonic Lamb shift results. Our fit averages over the systematic meanderings in the data set, which are different for each spectrometer. Overfitting to accommodate them easily biases the extrapolated slope at the origin. Solving this fitting conundrum will require independent confirmation of the shape of G_E from other electron or muon scattering measurements, which are underway or in planning [56–59]. In addition, a host of other relevant experiments are also underway or under analysis, including the completed but not yet published measurements of nuclear radii in other muonic atoms [60], and new high precision atomic level splitting experiments that will yield new and precise measurements of the proton radius [61–64]. We eagerly await all the new measurements that can elucidate the proton radius quandary.

[1] E. Chambers and R. Hofstadter, Phys.Rev. **103**, 1454 (1956).
[2] R. Pohl, R. Gilman, G. A. Miller, and K. Pachucki, Ann.Rev.Nucl.Part.Sci. **63**, 175 (2013), 1301.0905.
[3] C. E. Carlson, Prog.Part.Nucl.Phys. **82**, 59 (2015), 1502.05314.
[4] P. J. Mohr, B. N. Taylor, and D. B. Newell, Rev.Mod.Phys. **84**, 1527 (2012), 1203.5425.
[5] The 2014 CODATA recommended values are available at http://physics.nist.gov/cuu/Constants/index.html .
[6] J. Bernauer et al. (A1 Collaboration), Phys.Rev.Lett. **105**, 242001 (2010), 1007.5076.
[7] J. C. Bernauer et al. (A1), Phys. Rev. **C90**, 015206 (2014).
[8] J. Bernauer, P. Achenbach, C. Ayerbe Gayoso, R. Bohm, D. Bosnar, et al., Phys.Rev.Lett. **107**, 119102 (2011).
[9] R. Pohl, A. Antognini, F. Nez, F. D. Amaro, F. Biraben, et al., Nature **466**, 213 (2010).
[10] A. Antognini, F. Nez, K. Schuhmann, F. D. Amaro, F. Biraben, et al., Science **339**, 417 (2013).
[11] D. Tucker-Smith and I. Yavin, Phys. Rev. **D83**, 101702 (2011).
[12] B. Batell, D. McKeen, and M. Pospelov, Phys. Rev. Lett. **107**, 011803 (2011), 1103.0721.
[13] V. Barger, C.-W. Chiang, W.-Y. Keung, and D. Marfatia, Phys. Rev. Lett. **108**, 081802 (2012), 1109.6652.
[14] C. E. Carlson and B. C. Rislow, Phys. Rev. **D86**, 035013 (2012).
[15] C. E. Carlson and B. C. Rislow, Phys. Rev. **D89**, 035003 (2014).
[16] S. D. Glazek, Phys. Rev. **D90**, 045020 (2014), 1406.0127.

[17] G. Simon, C. Schmitt, F. Borkowski, and V. Walther, Nucl.Phys. **A333**, 381 (1980).
[18] I. Sick, Can.J.Phys. **85**, 409 (2007).
[19] I. Sick, Phys.Lett. **B576**, 62 (2003), nucl-ex/0310008.
[20] I. Sick and D. Trautmann, Phys.Rev. **C89**, 012201 (2014).
[21] M. Jones et al. (Jefferson Lab Hall A Collaboration), Phys.Rev.Lett. **84**, 1398 (2000), nucl-ex/9910005.
[22] O. Gayou et al. (Jefferson Lab Hall A Collaboration), Phys.Rev.Lett. **88**, 092301 (2002), nucl-ex/0111010.
[23] A. Puckett, E. Brash, M. Jones, W. Luo, M. Meziane, et al., Phys.Rev.Lett. **104**, 242301 (2010), 1005.3419.
[24] V. Punjabi, C. Perdrisat, K. Aniol, F. Baker, J. Berthot, et al., Phys.Rev. **C71**, 055202 (2005), nucl-ex/0501018.
[25] A. Puckett, E. Brash, O. Gayou, M. Jones, L. Pentchev, et al., Phys.Rev. **C85**, 045203 (2012), 1102.5737.
[26] I. Lorenz, H.-W. Hammer, and U.-G. Meissner, Eur.Phys.J. **A48**, 151 (2012), 1205.6628.
[27] I. T. Lorenz and U.-G. Meiner, Phys. Lett. **B737**, 57 (2014).
[28] G. Ron et al. (Jefferson Lab Hall A Collaboration), Phys.Rev. **C84**, 055204 (2011), 1103.5784.
[29] G. Ron, Mod.Phys.Lett. **A26**, 2605 (2011).
[30] X. Zhan, K. Allada, D. Armstrong, J. Arrington, W. Bertozzi, et al., Phys.Lett. **B705**, 59 (2011), 1102.0318.
[31] G. Ron, J. Glister, and X. Zhan, Nucl.Phys. **A827**, 273C (2009).
[32] G. Ron, J. Glister, B. Lee, K. Allada, W. Armstrong, et al.,

Phys.Rev.Lett. **99**, 202002 (2007), 0706.0128.

[33] G. MacLachlan, A. Aghalarian, A. Ahmidouch, B. Anderson, R. Asaturian, et al., Nucl.Phys. **A764**, 261 (2006).

[34] C. B. Crawford et al., Phys. Rev. Lett. **98**, 052301 (2007).

[35] M. K. Jones et al., Phys. Rev. **C74**, 035201 (2006).

[36] M. Paolone et al., Phys. Rev. Lett. **105**, 072001 (2010), 1002.2188.

[37] S. Strauch et al. (Jefferson Lab E93-049), Phys. Rev. Lett. **91**, 052301 (2003), nucl-ex/0211022.

[38] M. Vanderhaeghen and T. Walcher, Nucl. Phys. News **21**, 14 (2011), 1008.4225.

[39] V. Punjabi, C. F. Perdrisat, M. K. Jones, E. J. Brash, and C. E. Carlson, Eur. Phys. J. **A51**, 79 (2015), 1503.01452.

[40] W. A. McKinley and H. Feshbach, Phys. Rev. **74**, 1759 (1948).

[41] P. Blunden, W. Melnitchouk, and J. Tjon, Phys. Rev. Lett. **91**, 142304 (2003), nucl-th/0306076.

[42] Y. Chen, A. Afanasev, S. Brodsky, C. Carlson, and M. Vanderhaeghen, Phys. Rev. Lett. **93**, 122301 (2004), hep-ph/0403058.

[43] A. V. Afanasev, S. J. Brodsky, C. E. Carlson, Y.-C. Chen, and M. Vanderhaeghen, Phys. Rev. **D72**, 013008 (2005).

[44] I. A. Rachek et al., Phys. Rev. Lett. **114**, 062005 (2015).

[45] D. Adikaram et al. (CLAS), Phys. Rev. Lett. **114**, 062003 (2015), 1411.6908.

[46] Z. Abidin and C. E. Carlson, Phys.Rev. **D77**, 037301 (2008).

[47] M. Gorchtein, Phys. Rev. **C90**, 052201 (2014), 1406.1612.

[48] O. Tomalak and M. Vanderhaeghen (2015), 1508.03759.

[49] M. Horbatsch and E. A. Hessels (2015), 1509.05644.

[50] G. Lee, J. R. Arrington, and R. J. Hill, Phys. Rev. **D92**, 013013 (2015), 1505.01489.

[51] J. Arrington and I. Sick (2015), preprint, 1505.02680.

[52] I. T. Lorenz, U.-G. Meiner, H. W. Hammer, and Y. B. Dong, Phys. Rev. **D91**, 014023 (2015), 1411.1704.

[53] K. M. Graczyk and C. Juszczak, Phys. Rev. **C90**, 054334 (2014), 1408.0150.

[54] D. W. Higinbotham, A. A. Kabir, V. Lin, D. Meekins, B. Norum, and B. Sawatzky (2015), 1510.01293.

[55] R. J. Hill and G. Paz, Phys.Rev. **D82**, 113005 (2010).

[56] R. Gilman et al. (2013), MUSE Collaboration, 1303.2160.

[57] A. Gasparian et al. (2011), proposal JLab PR12-11-106.

[58] M. Mihovilovič, H. Merkel, and the A1-Collaboration, in *American Institute of Physics Conference Series, Vol. 1563*, edited by R. Milner, R. Carlini, and F. Maas (2013), pp. 187–190.

[59] Electron-deuteron elastic scattering, at Mainz, Michael Distler and Keith Griffioen, private communication.

[60] The published CREMA measurements are for muonic hydrogen [9, 10]. CREMA also measured transitions in muonic deuterium, ^{3}He, and ^{4}He, which are presently being analyzed.

[61] A. Vutha, N. Bezginov, I. Ferchichi, M. George, V. Isaac, C. Storry, A. Weatherbee, M. Weel, and E. Hessels (2012), BAPS.2012.DAMOP.D1.138.

[62] A. Beyer, C. G. Parthey, N. Kolachevsky, J. Alnis, K. Khabarova, R. Pohl, E. Peters, D. C. Yost, A. Matveev, K. Predehl, et al., J. Phys. Conf. **467**, 012003 (2013).

[63] O. Arnoult, F. Nez, L. Julien, and F. Biraben, European Physical Journal D **60**, 243 (2010), 1007.4794.

[64] J. Flowers, P. Baird, L. Bougueroua, H. Klein, and H. Margolis, IEEE Trans. Inst. Meas. **56**, 331 (2007).